Climate change impacts on summer flood frequencies in two mountainous catchments in China and Switzerland

S. Ragettli, X. Tong, G. Zhang, H. Wang, P. Zhang and M. Stähli

ABSTRACT

Flood events are difficult to characterize if available observation records are shorter than the recurrence intervals, and the non-stationarity of the climate adds additional uncertainty. In this study, we use a hydrological model coupled with a stochastic weather generator to simulate the summer flood regime in two mountainous catchments located in China and Switzerland. The models are set up with hourly data from only 10–20 years of observations but are successfully validated against 30–40-year long records of flood frequencies and magnitudes. To assess the climate change impacts on flood frequencies, we re-calibrate the weather generator with the climate statistics for 2021–2050 obtained from ensembles of bias-corrected regional climate models. Across all assessed return periods (10–100 years) and two emission scenarios, nearly all model chains indicate an intensification of flood extremes. According to the ensemble averages, the potential flood magnitudes increase by more than 30% in both catchments. The unambiguousness of the results is remarkable and can be explained by three factors rarely combined in previous studies: reduced statistical uncertainty due to a stochastic modelling approach, hourly time steps and the focus on headwater catchments where local topography and convective storms are causing runoff extremes within a confined area.

Key words | China, climate change, flood frequency, headwater catchments, stochastic modelling, Switzerland

S. Ragettli
H. Wang
Hydrosolutions Ltd.,
Winkelriedstrasse 5, Zurich 8006,
Switzerland

X. Tong (corresponding author)
G. Zhang
P. Zhang
Changjiang River Scientific Research Institute,
Huangpu Street No 23, Jiangan District, Wuhan City 430010,
China
E-mail: *ckytxx@163.com*

M. Stähli
Swiss Federal Institute for Forest,
Snow and Landscape Research WSL,
Zürcherstrasse 111, Birmensdorf 8903,
Switzerland

INTRODUCTION

Floods are a common risk in many mountainous areas worldwide. The estimations of flood magnitudes and return periods are an important issue for local water resources and risk management. However, the common length of the time series of peak flows is usually insufficient to obtain reliable extreme event estimations (Serinaldi & Kilsby 2015; van der Wiel *et al.* 2019). On the other hand, the use of long historical records for the flood frequency analysis brings in the question of flood stationarity since climatic and land-use conditions can affect the relevance of past flooding as a predictor of future flooding (Milly *et al.* 2005; Machado *et al.* 2015). Non-stationarity of the climate is even more an issue when future flood risks need to be estimated. Mitigation measures for future floods are usually planned without making assumptions regarding the impact of climate change (Olsen 2006; Rosenberg *et al.* 2010; François *et al.* 2019). A growing number of studies claim that this practice is no longer safe as, for many areas in the world, climate change impact studies project substantial increases in precipitation extremes (Fischer *et al.* 2013; Madsen *et al.* 2014; Westra *et al.* 2014) and in flood risks (Allamano *et al.* 2009; Hirabayashi

doi: 10.2166/nh.2019.118

et al. 2013; Alfieri et al. 2015; Arnell & Gosling 2016; Gu et al. 2018).

If long observation records from periods with a stationary climate are missing, weather generators can be used to generate hundreds of years of synthetic data, reflecting a wide set of climate statistics over a range of temporal scales (Fatichi et al. 2011). The historical statistics required to calibrate weather generators are calculated over time scales where climate stationarity can be assumed (Wilks & Wilby 1999). The long time series of precipitation obtained from weather generators have been used in extreme rainfall analysis (Hashmi et al. 2011; Peleg et al. 2017a, 2017b) and in hydrological models for flood risk estimation (Wheater et al. 2005; Paschalis et al. 2014).

Most studies about climate change impacts on flood frequency assume stationary climatic conditions within a given time window for the current and future climate (Madsen et al. 2014). Flow series representative of current and future conditions are simulated by a hydrological model, and then the change in discharge magnitude with a given return period is assessed based on flood frequency analysis (Prudhomme et al. 2003; Dankers & Feyen 2008, 2009; Arnell & Gosling 2016). Downscaling and bias correction methods are often applied to obtain the suitable input data time series from climate models. Stochastic weather generators can be useful for this purpose: stochastic downscaling of climate model projections aims at generating synthetic spatio-temporal weather data with statistical properties that are consistent with locally observed historical statistics – plus a factor of change computed from the control and future climate model outputs (Bordoy & Burlando 2014a, 2014b). Stochastic downscaling thus bridges the gap between the large-scale atmospheric states simulated by climate models and the local weather pattern observed at meteorological stations. Sunyer et al. (2012) compared five statistical downscaling methods for obtaining time series of future precipitation and concluded that weather generators are the most suitable method for downscaling when extreme events are the main focus. Hashmi et al. (2011) and Mekonnen & Disse (2018) have proved the good abilities of weather generators to simulate the frequency of observed extreme precipitation events of the current climate and for downscaling of future extreme events. Moreover, several studies have already used weather generators to assess the climate change impact on flood frequency (te Linde et al. 2010; Khazaei et al. 2012; Camici et al. 2014; Almasi & Soltani 2017; Gao et al. 2018; Keller et al. 2019). However, applications in small- and medium-sized catchments (<1,000 km^2) are still scarce.

One reason for the lack of such studies is data scarcity. Long runoff records from headwater catchments are required to validate simulated flood frequencies, but they are usually unavailable in mountain areas. Another reason is that the short response time of steep headwater catchments to extreme rainfall requires data at a fine time resolution to model peak discharges (Marchi et al. 2010). However, until recently, the available climate models did only provide monthly or daily rainfall outputs, which further complicated the downscaling of future extreme events. The questions regarding the significance of potential flood regime changes in mountain areas remain thus mostly unsolved. The direction of change reported in the available studies often depends strongly on the climate model and which the climate scenario is considered (e.g., Camici et al. 2014).

In this study, we assess the potential of a stochastic weather generator coupled with a continuous hydrological model in outweighing the drawback of short flood observation periods. The assessment is carried out in two first-order catchments, the Guanshan catchment in central China and the Alptal catchment in Switzerland. Both catchments are heavily forested and mountainous and have experienced substantial flood damage in the last decades. On the other hand, they represent completely different climate zones: Guanshan features a subtropical monsoon climate and Alptal a subalpine temperate climate.

In China, major investments have been undertaken in recent years to strengthen meteorological and hydrological monitoring (CCCPC 2015; Zhai et al. 2017). We assess if the availability of such data in combination with a hydrological model and the latest climate change projections does permit an unambiguous interpretation of the climate change impacts on floods. We apply stochastic downscaling to an ensemble of Regional Climate Models (RCMs), considering two main climate scenarios (representative concentration pathways [RCPs]). The modelled flood frequencies for the current climate are first validated against available observed

flood frequencies and then compared to the flood regime simulated for the future period 2021–2050.

STUDY SITES AND DATA

The two catchments have been chosen for this study because they are both pilot mountain research catchments in China and Switzerland where a relatively dense network of rain gauges has already been installed 10–20 years ago. Records of summer peak flows are even available for 30 or more years.

The Guanshan catchment in the western Hubei province in South China (Figure 1(a)) is a part of the Yangtze River Basin and has an area of 320.45 km^2. The elevation ranges from 240 to 1656 m a.s.l. with a mean elevation of 690 m. The topography of the Guanshan catchment is characterized by relatively steep slopes on soft, weathered rocks. More than 80% of the catchment is covered by forest and grassland, of which the forest cover accounts about 71% (Table 1). The Guanshan catchment has a subtropical monsoon climate which is cold and dry in winter, while annual precipitation is concentrated in summer (Figure 2(a)). There are three precipitation stations within the catchment (recording since 2007) and one hydro-meteorological station at the outlet (recording since 1973, Table 2). The annual average precipitation of the Guanshan catchment is about 900 mm. Heavy rainfall during the summer monsoon season in this area is mainly caused by meso-scale synoptic systems modulated by local terrain (Ding 1992). On 5 August 2012, the Guanshan catchment suffered a catastrophic flood, which caused economic losses of 33.5 million dollars.

The Alptal catchment is located in the central Swiss pre-Alps south of Lake Zurich (Figure 1(b)). The catchment has an area of 46.4 km^2, an altitudinal range from 840 to 1898 m a.s.l. (Table 1) and is part of the Rhine River Basin. Downstream of the catchment, the river Alp flows into the river Sihl. The topography of the Alptal valley is rather smooth with slopes of 20–40°. Most of the area is covered by Gleysols with limited permeability and practically no deep infiltration of water. Typically for this pre-alpine landscape, the vegetation cover is highly heterogeneous with the forest of Norway spruce (*Picea abies*) and silver fir (*Abies alba*), covering approximately 50% of the catchment (Table 1). Located at the transition from the Swiss Plateau to the central Swiss Alps, precipitation in this area is abundant with a

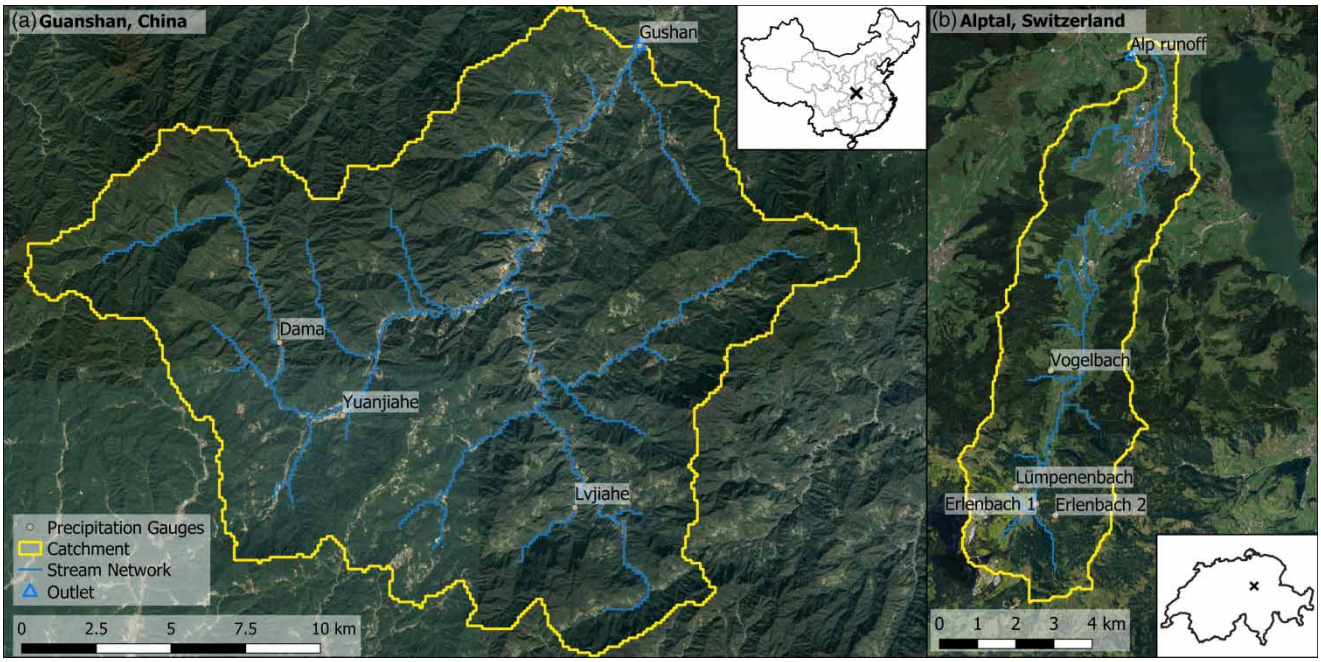

Figure 1 | Overview maps of the two study catchments. The locations of the available precipitation gauges and the hydrological stations at the outlet of the catchments are indicated. Google satellite imagery is used on the background.

Table 1 | Characteristics of study catchments

	Guanshan, China	Alptal, Switzerland
Outlet coordinates	110.93 E; 32.46 N	8.74 E; 47.15 N
Area	320.45 km^2	46.4 km^2
Mean elevation	690 m a.s.l.	1151 m a.s.l.
Elevation range	236–1656 m a.s.l.	840–1893 m a.s.l.
Mean slope	20.9°	15.2°
Forest cover (%)	71%	48.5%

distinct gradient from north to south (long-term average Einsiedeln: 1790 mm/year, Erlenbach: 2300 mm/year). The mean annual air temperature is 6.7 °C at the MeteoSwiss station in Einsiedeln. In normal winters, a closed snow cover of up to 2 m thickness is present from December to April. Runoff data from the gauge at Einsiedeln are available for the period 1991 until today. Precipitation has been recorded at four locations in the upper part of the catchment since 1999. Summer floods in the Alptal catchment can be both triggered by intense thunderstorms or long-lasting rainfall events.

METHODS

Hydrological model PRMS–Object Modelling System

The physically based, hydrological model Precipitation-Runoff Modelling System (PRMS; Leavesley & Stannard 1995; Leavesley *et al.* 2006) is used in this study. The model is implemented in the Java modelling framework Object Modelling System (OMS) (David *et al.* 2010). It has

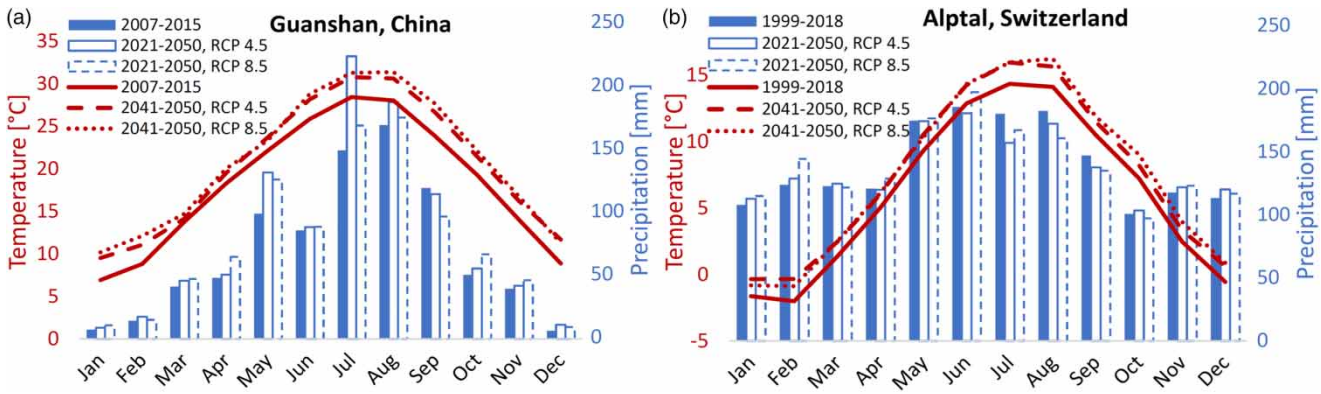

Figure 2 | Climate diagrams for (a) the Guanshan and (b) the Alptal catchment. Data from the Gushan station (Guanshan) and Erlenbach I (Alptal), respectively, are used for the precipitation profiles of the past period. Future temperature and precipitation profiles are extracted from the bias-corrected climate model data and represent ensemble average values.

Table 2 | Summary of available hydro-meteorological station data

	Guanshan, China			Alptal, Switzerland		
Variable	Station name	Elevation (m asl.)	Period	Station name	Elevation (m asl.)	Period
Hourly runoff	Gushan	236	2007–2015	Alp	850	1991–2018
Annual peak flows	Gushan	236	1973–2015	Alp	850	1991–2018
Hourly precipitation	Gushan, Lvjiahe, Dama and Yuanjiahe	236, 428, 456, 375	2007–2015 (Gushan: 1973–2015)	Vogelbach, Lümpenenbach and Erlenbach I and II	1100, 1180, 1100, 1210	1999–2018
Daily maximum/ minimum temperatures	County weather station	236	1973–2015	Erlenbach II	1210	1999–2018

been used recently for a multi-catchment modelling study in China by Ragettli *et al.* (2017), where the model was applied to simulate flash floods in 35 catchments in 10 Chinese provinces and where it demonstrated very good abilities in modelling the peak flows of flash floods in small- and medium-sized catchments (14–1,690 km^2) in South China, such as in the Hubei Province. Ragettli *et al.* (2017) have also introduced a new preprocessing tool for the model that is used for the division of the catchment into hydrologic response units (HRUs) and for the derivation of the river network from a digital elevation model (DEM). The HRUs are the smallest spatial units of the model and share topographic and hydraulic properties (see the section 'Model preprocessing and calibration'). The meteorological inputs required by PRMS–OMS are the time series of precipitation, as well as the maximum and minimum temperatures per time step.

PRMS–OMS can operate at both daily and hourly time steps. A higher temporal resolution is used during a 'storm mode' to simulate storm response in greater detail (Yates *et al.* 2000). The storm mode is activated when daily precipitation at any rain gauge within the catchment exceeds 5 mm. The model returns to the daily mode sequence if this threshold is not exceeded for two consecutive days (Ragettli *et al.* 2017). During the daily mode, the channel flow is not modelled explicitly, but all fluxes are conceptualized as a linear reservoir system. During the storm mode, a kinematic wave approximation is used for surface and channel flow routing. Infiltration, soil–water storage and water movement in the soil are also modelled in greater detail during the storm mode (see Ragettli *et al.* 2017 for more detail). The snow component of PRMS–OMS, on the other hand, is used only during the daily mode. We have therefore deactivated the storm mode for the months November to April (the period with potential snow influence) in this study and focus only on storm events in the months from May to October.

Model preprocessing and calibration

For the Guanshan catchment, we used the SRTM 3-arcsec DEM resampled to 100 m and flow accumulation to delineate the watershed and to map the channel network. In Alptal, we used the DHM25 DEM for Switzerland resampled to 50 m resolution. This resolution was still not sufficient for the flow accumulation algorithm to correctly identify the hydrological separation of the lake Sihl from the Alptal (the watershed divide lies only about 4 m higher than the level of the lake). We therefore manually edited the DEM at the water divide to obtain the correct watershed delineation.

The number of HRUs per catchment in PRMS–OMS depends on the drainage density because HRUs are defined as the flow contributing areas left and right of each channel segment. Channel segments are separated by channel nodes. The drainage density is thus the most important preprocessing variable and is controlled over the maximum area that may drain into a single channel grid cell. To estimate this parameter, we compared available river network maps to our generated maps (Figure 1). For the Guanshan catchment, we chose a maximum drainage area of 3 km^2 and for the Alptal a value of 0.8 km^2. This resulted in 118 HRUs and 75 channel segments in the Guanshan catchment and 61 HRUs and 39 channel segments in the Alptal catchment. Regarding the precipitation distribution, each HRU can only obtain precipitation inputs from one measurement station. We used the Thiessen polygon method to identify the nearest rain gauge of each HRU.

PRMS–OMS is calibrated against hourly discharge measured at the outlet of the catchment using the Nash–Sutcliffe efficiency criterion (NSE). The model consists of more than 20 parameters, but only five particularly sensitive model parameters are calibrated. For all other model parameters, constant empirical values are used or the values are estimated based on available channel, soil or land-use information. The five calibration parameters are identical as in Ragettli *et al.* (2017) and are listed in Table 3. The calibrated values are set to be constant in space and time. We apply the shuffled complex evolution (SCE) algorithm (Duan *et al.* 1993), an optimization algorithm widely used in hydrology for calibrating hydrological models, to fit PRMS–OMS to the observations. Because of the focus of this study on summer floods, only the hourly records during the active storm mode are used for calibration.

Spatio-temporal Neyman–Scott rectangular pulses weather generator

The spatio-temporal Neyman–Scott Rectangular Pulses (ST-NSRP) weather generator implemented in the RainSim

Table 3 | Model parameters

Parameter	Description	Unit
ST-NSRP (weather generator)		
Lambda	Mean waiting time between adjacent storm origins	h
Beta	Mean waiting time for raincell origins after storm origin	h
Rho	Spatial density of raincell centres	km^{-2}
Eta	Mean duration of a raincell	h
Xi	Mean intensity of a raincell	mm/h
Gamma	Mean radius of a raincell	km
PRMS–OMS (hydrological model)		
kpar	Hydraulic conductivity of the transmission zone (infiltration module)	mm/h
psp	Product of capillary rise and moisture deficit at the field capacity (infiltration module)	mm
soil_moist_max	Maximum available water holding capacity of the soil profile (subsurface component)	mm
ssr2gw_rate	Coefficient to route water from subsurface reservoirs to groundwater reservoirs (subsurface and groundwater component)	%/day
ssrcoef_lin	Coefficient to route subsurface storage to streamflow (subsurface routing)	–

software (Burton *et al.* 2008) is used in this study to generate hourly precipitation time series. The ST-NSRP model (Cowpertwait 1995; Cowpertwait *et al.* 2002) is a stochastic model that represents the spatial variability of precipitation as clusters of overlapping precipitation cells, each one characterized by a constant and homogeneous precipitation intensity. The spatio-temporal distribution of cells across a region is described through several stochastic processes. The simulated total precipitation depth at a particular coordinate and time is the sum of the intensities of all the active cells. Further details of the storm generation process ST-NSRP are provided by Burton *et al.* (2008) and by Bordoy & Burlando (2014a). In comparison to other weather generators available in the literature, ST-NSRP was assessed to be particularly strong in preserving observed spatial rainfall information (Vallam & Qin 2016). ST-NSRP has been applied in several climate change impact studies, including studies on future streamflow seasonality (Ragettli *et al.* 2013, 2016; Fatichi *et al.* 2015) and on future hydrological extremes (Khazaei *et al.* 2012; Camici *et al.* 2014).

The ST-NSRP model has six parameters presented and described in Table 3. The model parameters are optimized on a monthly basis, i.e., separately for each month of a record, using the SCE algorithm (Duan *et al.* 1993). To account for the precipitation signature across a continuum of scales, precipitation properties at several temporal scales are used to estimate the parameters. The following statistics at each station and per each month are considered in this study: (1) daily mean, (2) daily variance, (3) daily skewness, (4) daily auto-correlation lag-1, (5) the probability of dry day (defined as a day with precipitation <1 mm), (6) hourly variance and (7) hourly skewness, jointly with (8) all the cross-correlations between pairs of stations. This results in 7×12 months $= 84$ statistics for each of the four stations, plus $6 \times 12 = 72$ station cross-correlations per study catchment. The influence of each statistic on the fitting procedure is controlled by a vector of weights which distributes the fitting errors in inverse proportion to the weights (Burton *et al.* 2008).

It has to be noted that the ST-NSRP model can only be used to generate a stochastic time series of precipitation and at present cannot be coupled with a generator of air temperature time series. The air temperature has only a minor influence on summer flood extremes in the two study areas, mostly by affecting the initial wetness conditions in the catchments. We therefore did not set up a stochastic generator of air temperatures, but we randomly sampled air temperature time series from the historical records and from debiased climate model outputs, respectively.

RCM data and downscaling

The RCMs used in this study are provided through the European and the East-Asian branches of the international Coordinated Regional climate Downscaling Experiment (CORDEX) initiative (Giorgi *et al.* 2009). The purpose of the CORDEX initiative is to provide a quality-controlled dataset of downscaled information for the past and for future climate changes. In contrast to forcing with a general circulation model (GCM), RCMs provide information on much smaller scales within continental domains. Initial and boundary conditions are provided to the RCMs by the driving GCMs (Table 4).

The CORDEX models provide simulations for a period in the past (1970–2005) and at least two types of 45-year simulations for the future (2006–2050). For the future climate simulations, two scenarios (RCP 4.5 and RCP 8.5) are considered in this study. The RCP 8.5 scenario is characterized by increasing greenhouse gas emissions over time and therefore increasing greenhouse gas concentration levels and radiative forcing (Riahi *et al.* 2011). RCP 4.5 is a scenario that stabilizes radiative forcing at 4.5 $W m^{-2}$ in the year 2100 without ever exceeding that value (Thomson *et al.* 2011). For both the East-Asian and the European domain 5 RCMs are available per RCP (Table 4). The boundary conditions of the East-Asian RCPs are all obtained from the HadGEM2-AO GCM, while the European CORDEX ensemble considered several driving GCMs (Table 4). The entire available ensemble for Alptal consists of 13 RCM–GCM combinations for RCP 4.5 and 17 for RCP 8.5.

Reparameterization of ST-NSRP

The methodology to downscale climate model outputs to high-resolution climate precipitation scenarios in this study follows the approach presented in Bordoy & Burlando (2014b). It consists of the steps schematized in Figure 3 and can be summarized as follows. The first step is to debias the climate model outputs. Then, the precipitation statistics are computed for the control period in the past (1989–2018) and for the future period 2021–2050. Next, the factors of change are computed (α_i) and used to perturb the observed statistics (K_i), in order to obtain future statistics (S_i). A new set of ST-NSRP model parameters is obtained for future statistics and, finally, the model is used to simulate the synthetic precipitation time series for the future climate. The scaling properties of the raw moments of the observed records are used to scale down S_i^{daily} to hourly resolution, but only for the

Table 4 | RCMs used in this study

RCM	GCMs for boundary conditions	Temporal resolution	Spatial resolution
Guanshan catchment, China			
HadGEM3-RA	HadGEM2-AO	3-h, 1 day	0.44°
RegCM4	HadGEM2-AO	3-h, 1 day	50 km
SNU-MM5	HadGEM2-AO	3-h, 1 day	50 km
SNU-WRF	HadGEM2-AO	3-h, 1 day	50 km
YSU-RSM	HadGEM2-AO	3-h, 1 day	50 km
Alptal catchment, Switzerland			
CLMcom-CCLM4-8-17	HADGEM-EUR44	1 day	0.44°
CLMcom-CCLM5-0-6	ECEARTH-EUR44, HADGEM-EUR44, MIROC-EUR44, MPIESM-EUR44	1 day	0.44°
DMI-HIRHAM5	ECEARTH-EUR11, ECEARTH-EUR44	1 day	0.11°, 0.44°
KNMI-RACMO22E	ECEARTH-EUR44, HADGEM-EUR44	1 day	0.44°
SMHI-RCA4	CCCMA-EUR44, ECEARTH-EUR11, ECEARTH-EUR44, HADGEM-EUR11, HADGEM-EUR44, MIROC-EUR44, MPIESM-EUR11, MPIESM-EUR44, NORESM-EUR44	1 day	0.11°, 0.44°

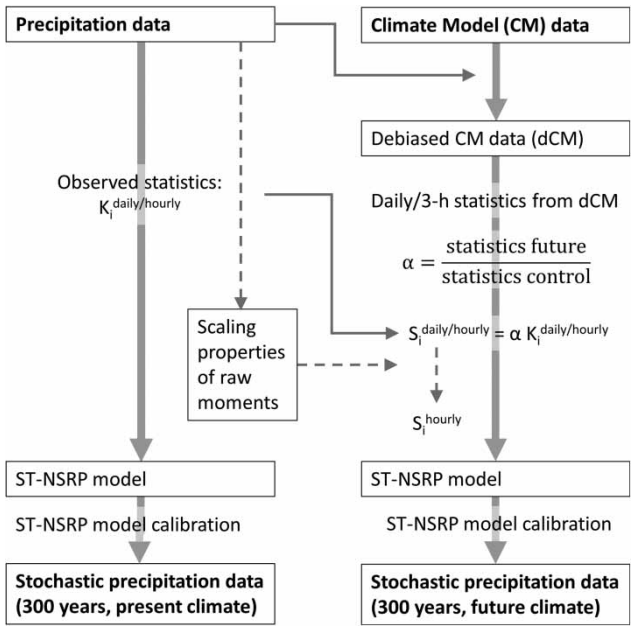

Figure 3 | Design of the stochastic downscaling procedure (adapted from Bordoy & Burlando 2014a, 2014b).

special case when the RCM outputs are available only at daily resolution and therefore the factor α of the required hourly statistics (i.e., hourly variance and skewness) cannot be computed directly from the RCM outputs.

The use of observed statistics perturbed by a factor of change, rather than using directly the statistics of the RCMs, minimizes the propagation of multiplicative climate model errors (Bordoy & Burlando 2014b). However, bias correction of climate models is still recommended for adjusting the RCM outputs to the local climate characteristics. To debias precipitation outputs of RCMs for the Guanshan catchment, we apply non-parametric quantile mapping. For the Swiss catchment, we used the CH2018 climate scenarios for Einsiedeln (National Centre for Climate Services 2018) which have already been bias-corrected based on quantile mapping prior to this study. In quantile mapping, the RCM outputs are adjusted to the observed cumulative density functions of precipitation and temperature, respectively, by using tables of empirical percentiles. The method has been found to effectively reduce systematic errors in climate model outputs and has thus been recommended for most applications of statistical bias correction (Gudmundsson *et al.* 2012). The climate4R framework, implemented in the statistical software R, is used for all climate data post-processing steps in this study (Iturbide *et al.* 2019).

Precipitation outputs of RCMs provided through CORDEX East Asia are available at daily and 3-hourly resolution (Table 4). The factors of change α of the 3-hourly variance and skewness are used in this study as a proxy for the change in corresponding 1-hourly statistics. However, RCMs available for Alptal only provide daily precipitation outputs. Hourly statistics are obtained by making use of the scaling properties of the precipitation process, as observed from the scaling of the raw moments (Bordoy & Burlando 2014a, 2014b). We assume that the scaling properties of the raw moments remain unaltered under climate change. A discussion of that assumption and the methodology of raw moment scaling are provided by Bordoy & Burlando (2014b).

We assume that the observed cross-correlation between pairs of stations remains invariant under climate change. Indeed, because of the short distance between the stations in our catchments (in general less than 10 km), all stations fall in the same climate model grid cell and are thus characterized by the same signature change.

Model validation and flood frequency analysis

PRMS–OMS outputs are validated against two types of data in this study: (a) discharge during the storm mode of a period different from the calibration period and (b) the flood frequency curve as identified from historical records of annual peak flows. Unfortunately, due to limited data availability, the first option is only possible in the Alptal catchment. For the model calibration related to the Guanshan catchment, we used all available hourly runoff observations from 2007 to 2015. In South China, PRMS–OMS model performance has already been exhaustively assessed by Ragettli *et al.* (2017).

For the validation of simulated storm flows against observed hourly records in the Alptal catchment, the model is forced with measured inputs of precipitation and temperature. For the assessment of simulated flood frequencies, however, PRMS–OMS is forced with stochastic inputs provided through the ST-NSRP weather generator. The clear advantage of using the stochastic data is that much longer time series can be produced. We therefore generate the

300-year time series of runoff with each ST-NSRP reparameterization (both for the present and for the future climates).

The ability of PRMS–OMS to correctly identify streamflow extremes is assessed by comparing the generalized extreme value (GEV) distributions fitted to observed and simulated peak flows. Asadi *et al.* (2018) have found that the GEV distribution provides a good approximation to the extremes of river discharges in the Rhine basin in Switzerland. The GEV distribution has also been extensively used to estimate the return period of flood events in South China (Tian *et al.* 2016; Ragettli *et al.* 2017).

GEV fits are made under the assumption that the full distribution of extreme events can be described by a GEV function. This assumption may not always be valid, especially for rivers where different runoff generating processes can cause extreme events (van der Wiel *et al.* 2019). Fischer & Schumann (2019) found in Germany that flood events with a return period of 8 years or more are likely to be caused by different generating processes than flood events with a lower return period. Because the focus of this study is on floods with long recurrence intervals, we therefore fit the GEV distributions only to simulated events with a return period of at least 10 years according to the empirical probability distribution. This approach is equivalent to a peak-over-threshold (POT) analysis, where the threshold is set to the value of the 30th largest event in 300 simulation years. In order to ensure the independency of events, only 1 peak flow within 5 days is extracted from the model outputs for the POT analysis.

van der Wiel *et al.* (2019) have demonstrated that the uncertainties of a GEV fit to even 100 years of data can be so large that no significant flood regime change could be found, while a GEV fit to 2000 years showed a statistically significant increase in flood magnitudes. They argued that studies focussing on the impact of climatic changes on hydrological extremes should use such large ensemble techniques. However, 2000 years of runoff simulations for each RCM, RCP and catchment in our study would lead to computational constraints. As a compromise, we generate ensembles of 10 times 300 years of precipitation data with the weather generator. We then computed the median of the 1st, 2nd and 3rd until the 30th largest daily rainfall amount in 300 years and chose for the runoff simulations the ensemble member with the lowest root mean square difference with respect to the 30 median values. Our methodology thus ensures a robust statistical analysis of the climate change impact on simulated extreme flows.

Calculation of confidence intervals

For the estimation of uncertainty in fitted GEV distributions, we compute the profile likelihood function of the GEV parameters (i.e., the shape parameter ξ, the scale parameter σ and the location parameter μ) and then consider the 60% and 95% confidence intervals (CIs) of the maximum likelihood estimates. The profile likelihood method has been suggested as preferable for the estimation of uncertainty in distributions fitted to hydro-meteorological extremes (Serinaldi & Kilsby 2015). To assess the climate model ensemble uncertainty, we also compute the 60% and 95% CIs in the obtained flood magnitudes for a given return period.

RESULTS

Model calibration and validation

Deterministic model simulations

The automatic calibration of the PRMS–OMS model resulted in NSE values of 0.79 for the Guanshan catchment and 0.77 for the Alptal catchment, respectively (Figure 4). The mean volume error (ΔQ, not used for the calibration) is only 1% in Guanshan and 11% in Alptal. There was only one major flood event during the calibration period in Guanshan (5 August 2012, Figure 4(a)). To assess if the model realistically represents the runoff generation processes, we present the components of simulated runoff during this storm event in Figure 4(b). According to these results, subsurface flow represents 58%, surface runoff 41% and groundwater flow 1% of the total streamflow components. The runoff coefficient (total simulated discharge divided by total rainfall) was 0.76. We could finally not use the three stations in the upper part of the catchment (Figure 1) to force the model during the calibration because precipitation measured at these three stations during the 2012 storm event was less than the measured streamflow depth. If these had been used for the calibration, the

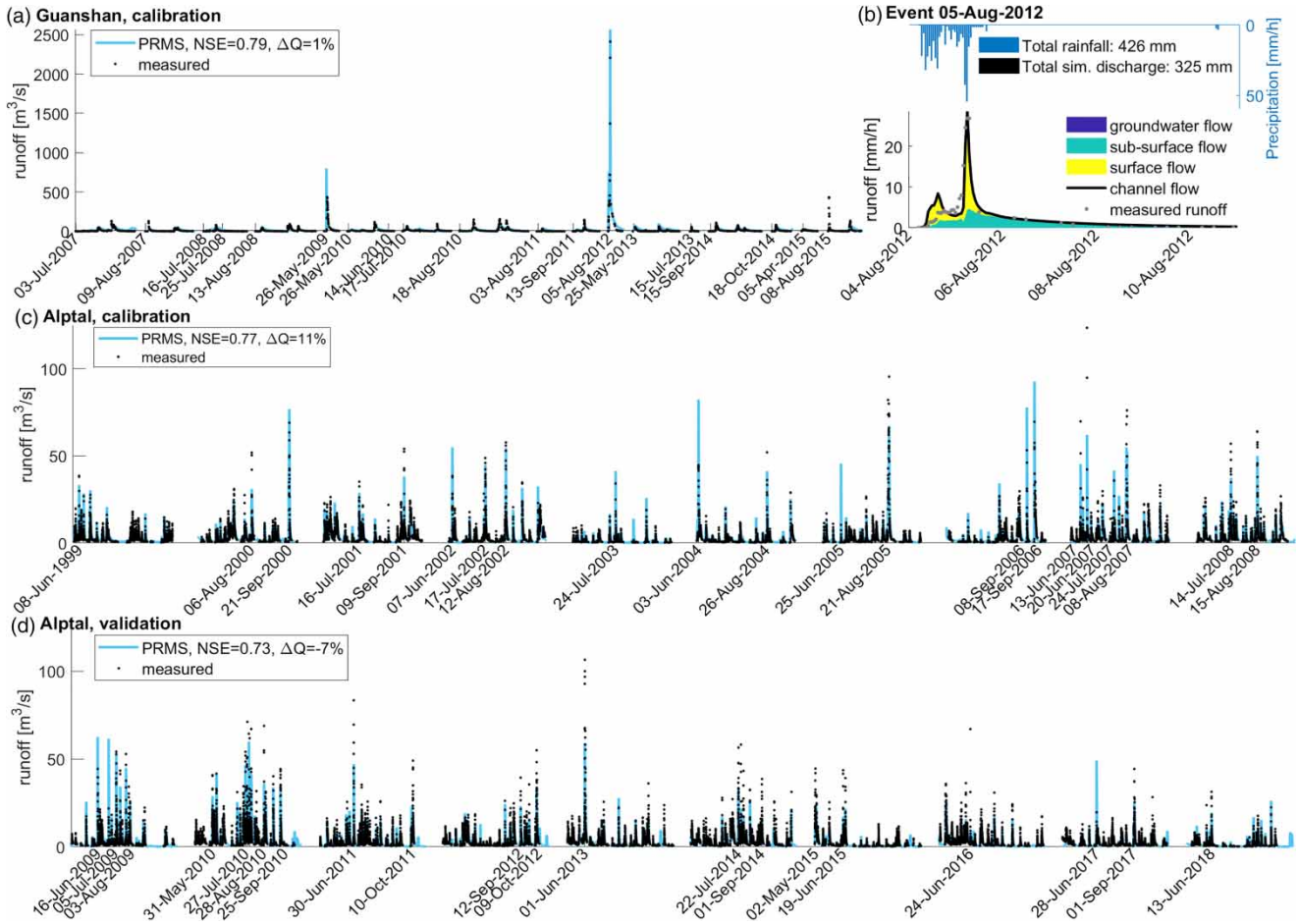

Figure 4 | Observed and simulated hourly runoff during storm events at Guanshan and Alptal catchments. (a) calibration period Guanshan (2007–2015), (b) precipitation, runoff and simulated flow components during the 5 August 2012 event in Guanshan, (c) calibration period Alptal (1999–2009), (d) validation period Alptal (2009–2018). NSE is the Nash–Sutcliffe efficiency and ΔQ is the total volume error.

automatic calibration would have led to a runoff coefficient of one and almost no subsurface flow contribution to streamflow. We considered this as highly unrealistic and an unfavourable parameterization of the model. Only Gushan station inputs were therefore used for the calibration.

The calibrated PRMS–OMS model for the Alptal catchment is validated against the observed runoff from all storm events during the period 2009–2018. The NSE value of 0.73 and the total volume error of −7% prove the good model skills in simulating storm flows (Figure 4(d)). However, the simulated peak flow during the largest floods recorded during the calibration and the validation periods (13 June 2007 and 1 June 2013, respectively) is only 50% and 55% of the measured peak discharge. An explanation for this could be that the available precipitation data may not represent well the rainfall patterns in the catchment during these events, similar to that in Guanshan during the August 2012 event. For other events, the model overestimates peak flows (e.g., 17 September 2006) or reproduces them accurately (e.g., 21 September 2000, Figure 4(d)). Overall, the results do not suggest that the model systematically over- or underestimates peak flows.

Stochastic model simulations

The station climate statistics (see Figures 5 and 6 for an example from each catchment) in combination with the

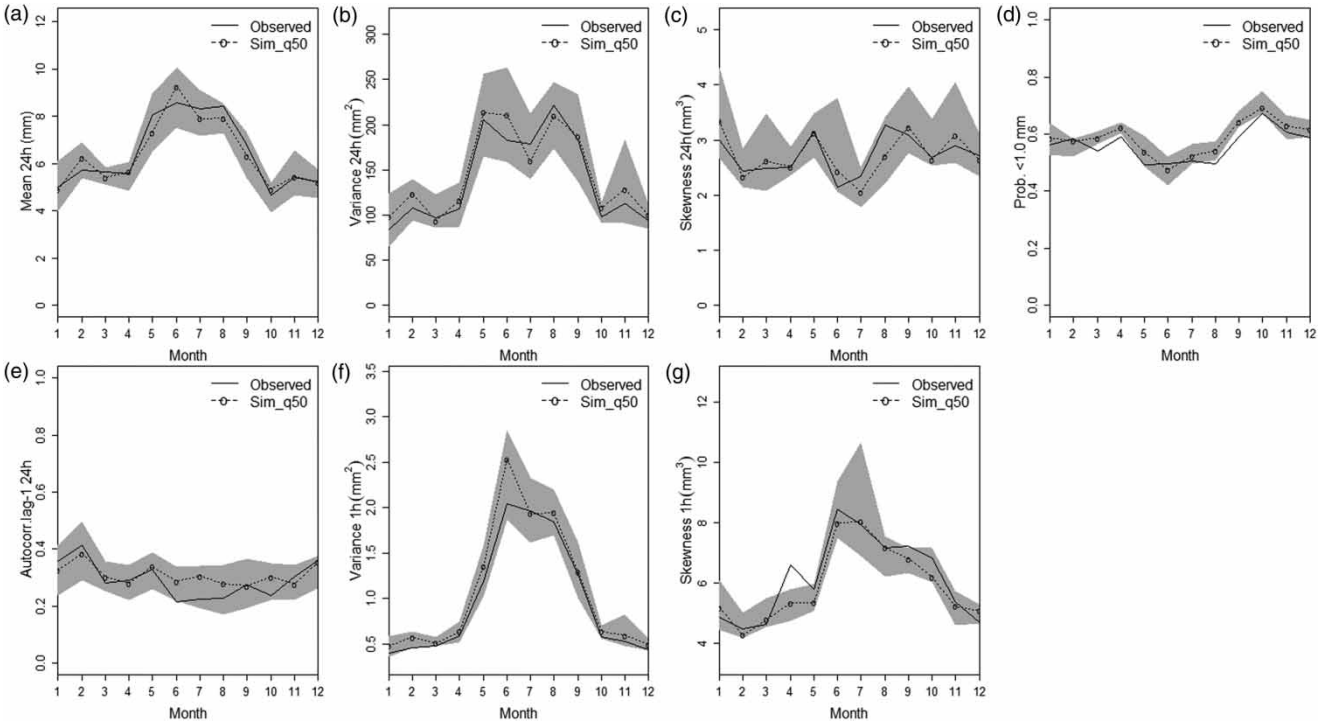

Figure 5 | Climate statistics of the Erlenbach I station in the Alptal catchment. The figure shows the observed statistics from the period 1999–2018 and the statistics as simulated by the ST-NSRP model for a 20-year period (dotted line: median statistics out of 10 Monte Carlo realizations, grey area: maximum and minimum statistics out of 10 Monte Carlo realizations).

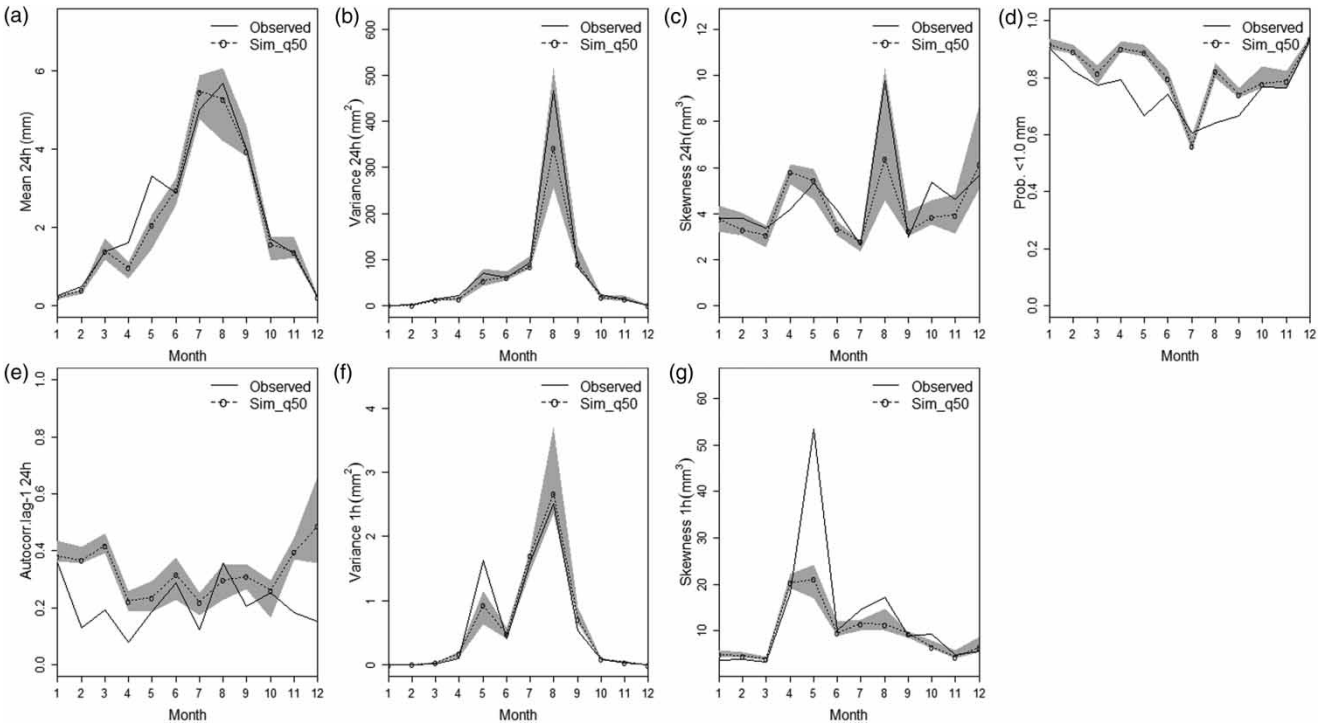

Figure 6 | Climate statistics of the Gushan station in the Guanshan catchment. The figure shows the observed statistics from the period 2007–2015 and the statistics as simulated by the ST-NSRP model for a 20-year period (dotted line: median statistics out of 10 Monte Carlo realizations, grey area: maximum and minimum statistics out of 10 Monte Carlo realizations).

observed cross-correlations between the four stations in each catchment are the basis for setting up the rainfall generation model ST-NSRP. The historical data from all the four stations per catchment still represent valuable information on the rainfall patterns in the catchment, even if they might not capture the total precipitation in the catchment during each of the events equally well (see the section above). The weather generator is able to reproduce the observed rainfall statistics well. In the Alptal catchment, at the station Erlenbach I, the observed statistics are entirely within the range of values obtained from 10 Monte Carlo runs (Figure 5). Only the dry probability is slightly overestimated in August and September (Figure 5(d)). The value of this statistic is also overestimated during most of the months at the Gushan station in the Guanshan catchment (Figure 6(d)). At the Gushan station, the model has difficulties in representing the climate statistics for the month of May (Figure 6). However, there may be an artefact in those data since the hourly skewness is more than 100% higher than in any other month. The allowed range of ST-NSRP parameters prevents the model from overfitting to such unrealistic values. Furthermore, the auto-correlation during the winter months is overestimated (Figure 6(e)), which is however not relevant here due to the focus on summer storm events.

The simulated flood frequency distribution with stochastic inputs is presented in Figure 7. The fitted GEV distribution of observed flows in Guanshan is entirely within the 60% CI of the GEV distribution fitted to the simulations (Figure 7(a)). According to the GEV distribution fitted to observations, the 2012 flood event is characterized by a recurrence interval of 76 years. According to the stochastic simulations, such an event occurs on average every 108 years (indicated by the dotted vertical lines in Figure 7(a)). Another extreme event that occurred in 1975 has a return period of 63 years according to observations and 88 years according to simulations, respectively. Given that the observation period was only 43 years, the GEV values for such large events should be treated with care. Indeed, the 60% CI is much larger than the differences in the return period estimates between observations and simulations (Figure 7(a)).

In Alptal, the simulated peak flows with a return period larger than 2 years exceed the flows as estimated from the observations. Events with a return period between 3 and 50 years are estimated on average 21% higher according to the GEV distribution of simulations. It is interesting to find that the plotting positions of the four largest observed flood events are all above the GEV flood frequency curve (Figure 7(b)). It is possible that the flood generation processes are different for such rare

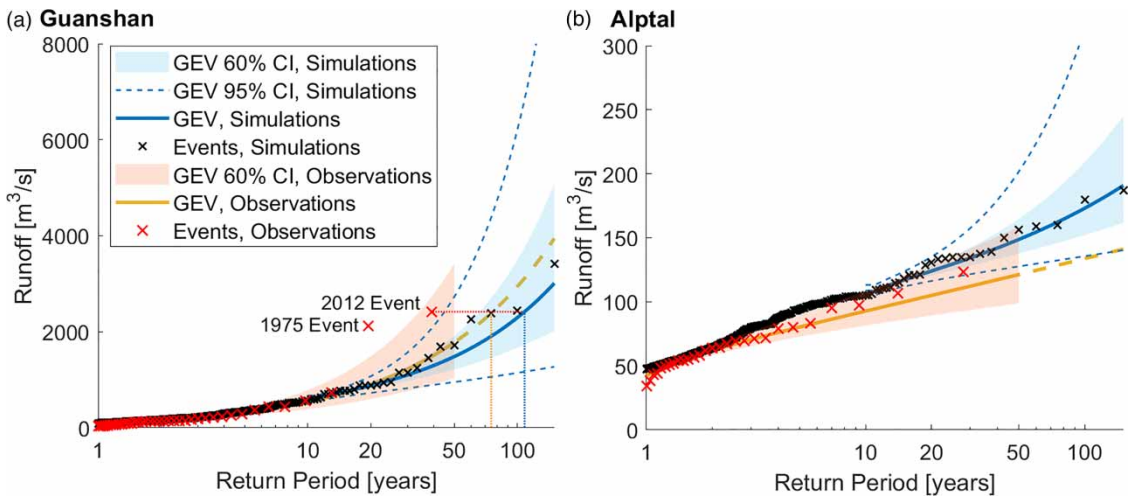

Figure 7 | Validation of return periods of peak flows at the Guanshan (a) and Alptal (b) rivers simulated by PRMS–OMS. The figure shows the return periods of observed and simulated hourly peak flows according to the empirical probability distribution (crosses) and the extreme value statistics (GEV). The return periods are calculated based on 43 years of the observed discharge (1973–2015) in Guanshan and 28 years (1991–2018) in Alptal, respectively, and based on the 300-year time series of stochastic simulations. The 60 and 95% CIs of the GEV fits are indicated.

events, and that they are therefore not well represented by the GEV distribution fitted to all annual peak flows. This possibility is taken into account by the GEV distribution of the stochastic outputs, which is fitted only to events with an empirical return period of 10 years or more (see the section 'Model validation and flood frequency analysis'). Furthermore, all these four events occurred during the period 1999–2018, which was also used for the calibration of the weather generator. If the empirical return period of the four events is calculated over the period 1999–2018 instead of 1991–2018, their plotting position is shifted to the left and consequently fit closely the distribution of the simulations. For example, a 20-year event in the Alptal catchment has a peak flow of 124.1 m^3/s according to the distribution of the simulations, which is almost identical to the peak flow of the largest event observed during the recent 20-year period (123.5 m^3/s, 20 June 2007). Our analysis thus underlines that the simulated flood frequencies from both catchments are plausible and can be used as a reference for the simulated future flood frequencies.

Climate statistics in 2021–2050

The range of climate statistics obtained from the bias-corrected RCM indicates a gradual increase in air temperatures in both catchments until 2050 (Figure 8). Compared to the period 2001–2010, the air temperatures in Guanshan are projected to increase by 1.6–2.2 °C until 2041–2050 according to the RCP 4.5 scenario, and by 2.7–2.9 °C following RCP 8.5. In Alptal, these values are 1.3–2.0 and 0.9–2.3 °C, respectively.

The bias-corrected and downscaled RCM ensembles available for the Guanshan catchment indicate an increase in mean annual summer precipitation by 8% (RCP 4.5, ensemble median) and 6% (RCP 8.5), respectively, comparing the future period 2021–2050 to the observation period 1989–2018 (Figure 9(a)). For the Alptal catchment, on the other hand, the RCM ensemble projects a decrease in summer precipitation (RCP 4.5: −7%, RCP 4.5: −4%; ensemble medians, Figure 9(d)). The patterns are different with respect to the expected changes in the daily variance and skewness. Regarding the variance, the RCMs do not indicate a clear direction of change, but almost all RCMs project and increase in the skewness of daily summer precipitation (Figure 9(e) and (f)). In Guanshan, as in Alptal, the ensemble median of the RCPs indicates an increase in the daily skewness by more than 10% (both RCPs, Figure 9(c)). High skewness values are associated with extreme precipitation and therefore point to an intensification of extremes. Projected changes in other statistics required by the weather generator such as the dry probability or the daily auto-correlation are not reported here for reasons of shortness and because their association with extreme precipitation or floods is less straightforward.

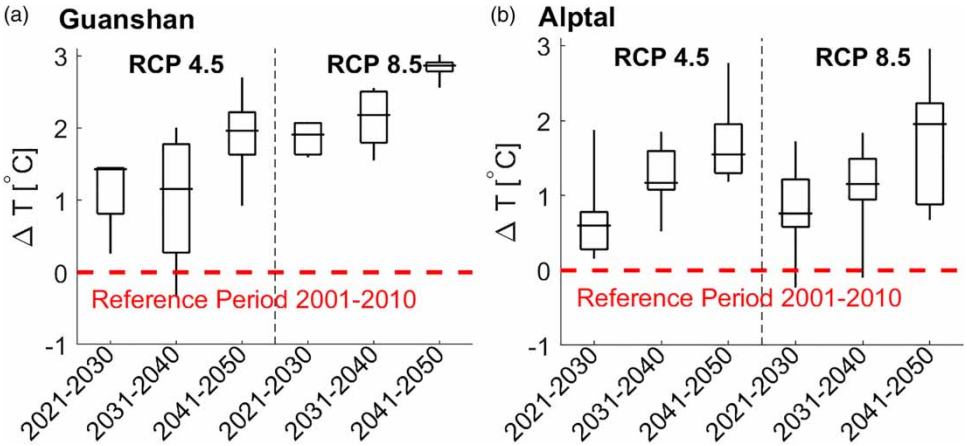

Figure 8 | Expected changes in average May–September daily maximum temperatures calculated from the bias-corrected RCM data. The changes are calculated between a reference period (2001–2010) and each decade between 2021 and 2050. The horizontal bars indicate the median of all RCMs for each RCP and study catchment. The boxes indicate the 25th and 75th percentiles, and whiskers indicate the maximum and minimum values.

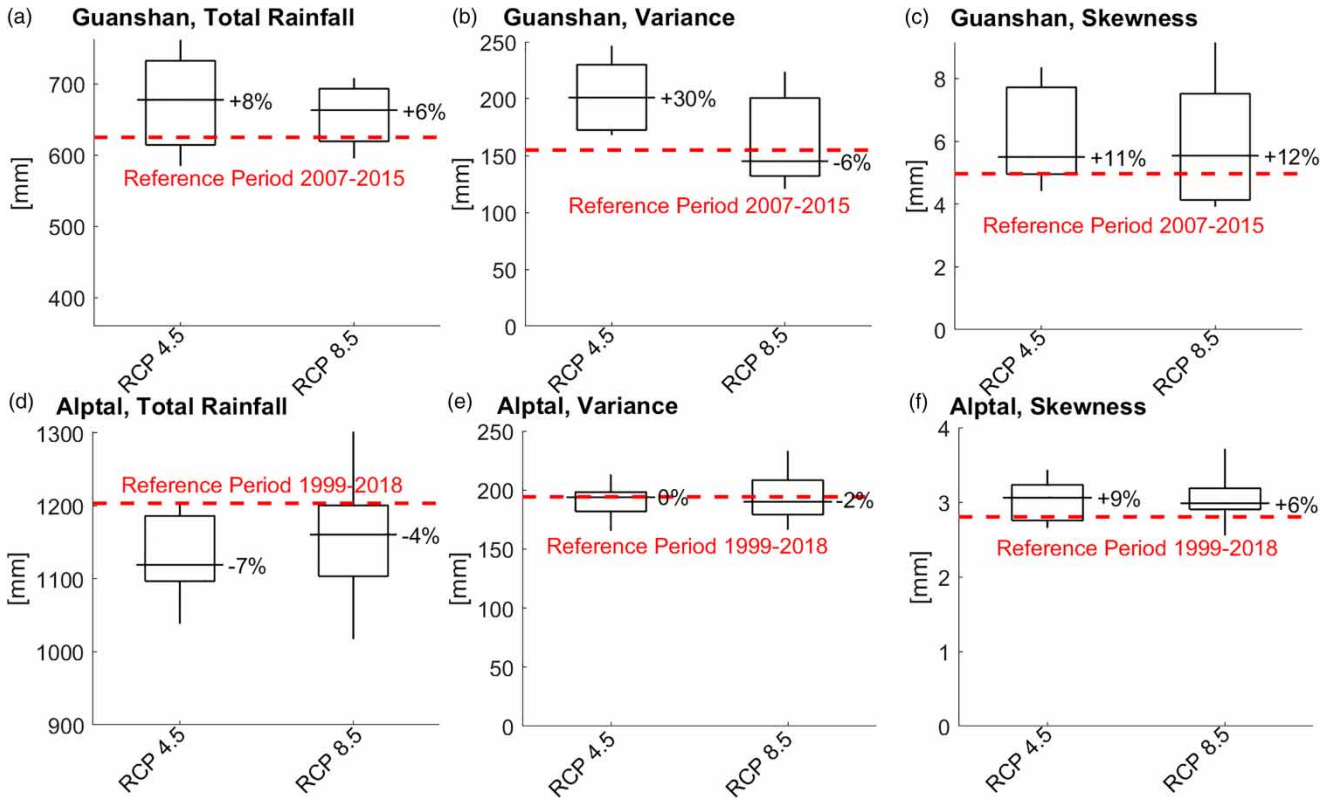

Figure 9 | May–September precipitation statistics (total rainfall, daily variance and skewness) of the observation period (2007–2015 in Guanshan, 1999–2018 in Alptal) and future period (2021–2050) as calculated from the bias-corrected and downscaled RCMs. The horizontal bars indicate the median of all RCMs for each RCP and study catchment. The boxes indicate the 25th and 75th percentiles, and whiskers indicate the maximum and minimum values.

Flood frequencies in 2021–2050

The ensemble average of both assessed scenarios (RCP 4.5 and RCP 8.5) and in both catchments points to a strong future increase in flood magnitudes and frequency (Figure 10). In the Alptal catchment, for both RCPs, the flood frequency curve obtained by GEV-fitting for the reference period is outside the 95% CI of the flood frequency curve identified for 2021–2050 (Figures 10(b) and (c)). The same is the case in Guanshan considering the RCP 4.5 scenario (Figure 10(a)). Indeed, in all these three cases, none of the individual RCMs from the ensemble projects a decrease in flood magnitudes and frequency. A decrease in extremes is possible in Guanshan according to two RCMs (RegCM and SNU, Table 4) for the RCP 8.5 scenario. In this latter case, the ensemble uncertainty of the climate models is so large that the 60% CI entirely overlaps with the 60% CI of the GEV distribution for the reference period (Figure 10(b)). However, also in this case, the ensemble average is still above the 60% CI of the reference period.

Generally, the model outputs for the future period indicate a stronger relative increase in the flood magnitude for very rare events. In the Alptal catchment, the peak flows of floods with a return period of 20 years are projected to increase by 25–50%, while the floods with a recurrence interval of 100 years increase by 60–90% according to the ensemble average (both RCPs, Figure 11(b)). In Guanshan, the projected relative changes are even stronger. The magnitude of a 20-year flood increases by about 60%, and the projected peak flows of a 100-year flood exceed the peak flows of a current 100-year flood by 100% (RCP 4.5, Figure 11(a)). Under RCP 8.5 conditions, the ensemble average for the Guanshan catchment projects an increase in the flood magnitude by about 45–60% across all return periods (Figure 11(a)). Considering the ensemble average, a 100-year flood in Guanshan of the reference period statistically

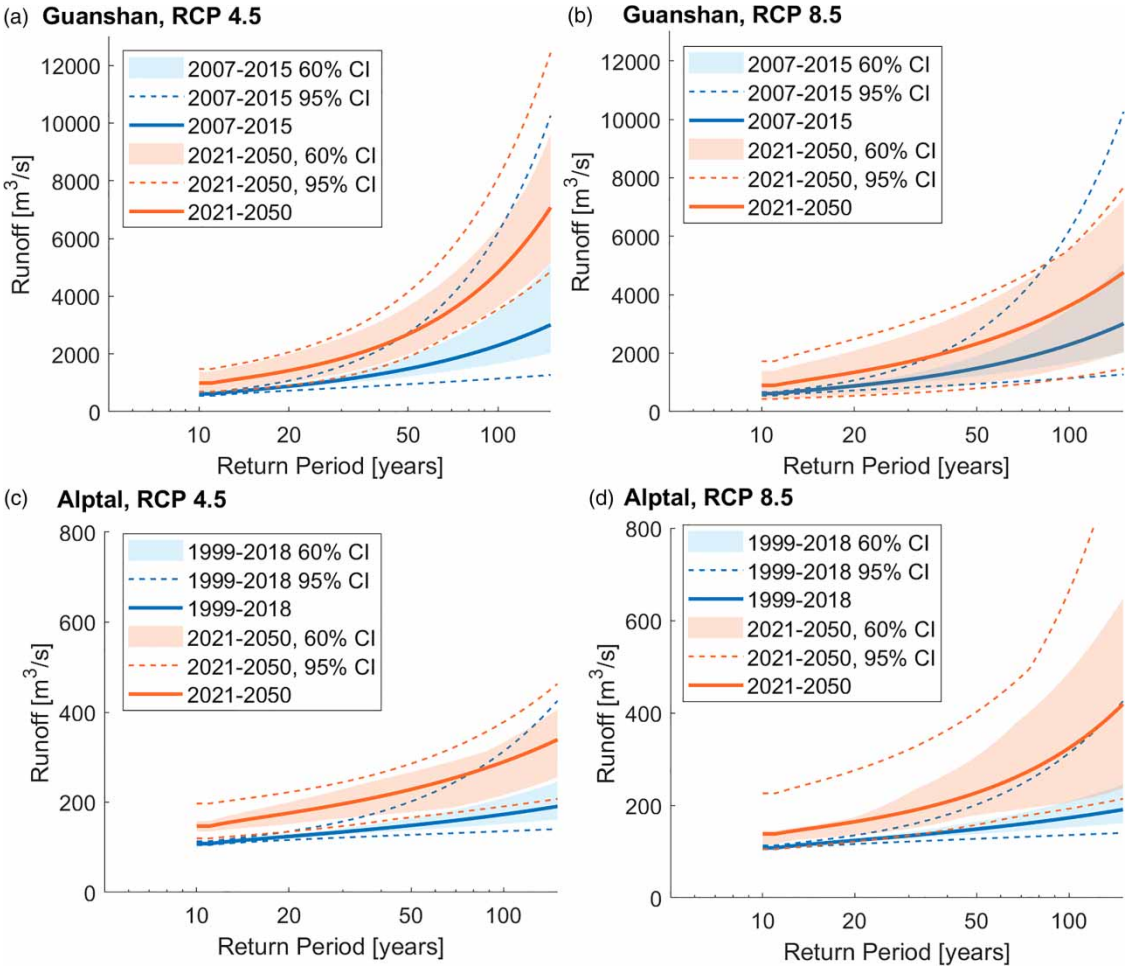

Figure 10 | Flood frequency curves for Guanshan (a and b) and Alptal (c and d) for the reference period (blue lines) and the future period 2021–2050 (red lines, two climate scenarios RCP 4.5 and RCP 8.5, ensemble averages). The figure shows the GEV distributions fitted to the simulated hourly peak flows from 300-year time series of stochastic runoff simulations. The uncertainty bounds for the reference period indicate the 60% and 95% CIs of the GEV fits, and the uncertainty bounds for the future period indicate the 60% and 95% CIs of the ensemble of fitted GEVs from all climate models. Please refer to the online version of this paper to see this figure in colour: http://dx.doi.org/10.2166/nh.2019.118.

occurs every 40–50 years in the future (both RCPs, Figures 10(a) and (b)). In the Alptal catchment, floods that are rated as 100-year floods under the current climate could even have a return period of 20–25 years in the future (both RCPs, ensemble average, Figures 10(c) and (d)).

DISCUSSION

Comparison with previous studies

In Switzerland, heavy precipitation events are projected to intensify in all seasons and regions (Rajczak & Schär 2017; Ban *et al.* 2018; National Centre for Climate Services 2018). The most substantial and widespread intensifications are projected to occur in the northern Alpine region (Rajczak *et al.* 2013; Gobiet *et al.* 2014), where also the Alptal catchment is located. A few studies have already provided evidence on recent increasing trends in annual daily maximum precipitation based on station data (Scherrer *et al.* 2016). Regarding floods, Köplin *et al.* (2014) projected increases in mean annual floods by 5–25% over most parts of Switzerland for the period 2025–2046. A trend detection based on historical data for Alpine catchments in Switzerland is not yet feasible due to short observational records and because extreme events are rare per definition (Gobiet *et al.* 2014; Andres & Badoux 2018). Our results agree with the sign of the changes in precipitation and runoff extremes,

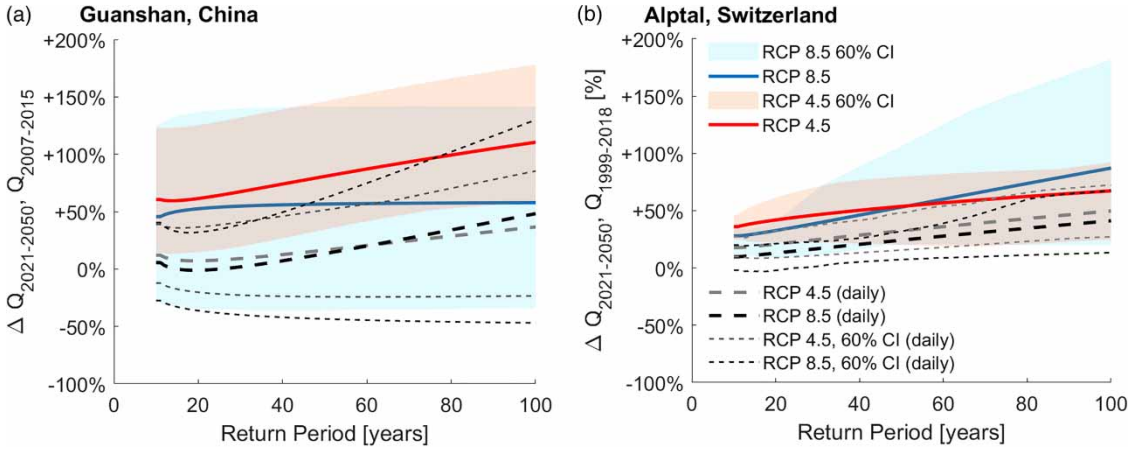

Figure 11 | Expected relative changes in peak flows for given return periods in Guanshan (a) and Alptal (b). The solid lines represent the climate model ensemble average (RCP 4.5 and RCP 8.5) regarding hourly peak flows, and the uncertainty bounds indicate the 60% and 95% CIs of the results obtained for each climate model. The dotted lines indicate the changes if the model outputs are aggregated to daily flows.

but because of differences in the study set-up, our results cannot be compared systematically to the above-listed studies. The findings about the mean temperature increases and precipitation decreases in summer in Alptal are consistent with earlier studies (Keller *et al.* 2017; Ban *et al.* 2018; National Centre for Climate Services 2018).

According to Zhang *et al.* (2008), precipitation intensity showed a significant increasing trend in the middle and lower Yangtze River Basin between 1960 and 2005. An evaluation of outputs from the same RCM ensemble as used in this study but for the whole Yangtze River Basin indicates for 2020–2049 an increase of mean summer precipitation by 4–6% (Gu *et al.* 2018). Gu *et al.* (2018) also modelled changes in streamflow at three mainstream stations in the Yangtze River Basin until 2020–2049. Maximum 1-day streamflow with a return period of 50 years was projected to increase by 8–17% (RCP 4.5) and by 15–22% (RCP 8.5), respectively, considering the ensemble average and the reference period 1980–2005. These projections of daily peak flow increases are similar to our ensemble average values identified for the Guanshan catchment (13–17% increases, daily values, Figure 11(a)). Gao *et al.* (2018) simulated the climate change impact on flood frequencies in two rivers in the lower Yangtze River Basin and showed that design runoffs and water levels indicate an increasing trend. All the above-mentioned studies have concluded that the reported changes in summer precipitation and river flows have the potential to result in a higher occurrence probability of flood hazards in the Yangtze River Basin, which is consistent with our findings.

For both regions in our study, the single-day precipitation and flood events are projected to intensify more than multi-day events (Rajczak *et al.* 2013; Rajczak & Schär 2017; Gu *et al.* 2018). Shorter sub-daily extremes have received much less attention, although they are projected to intensify even more (Ban *et al.* 2018). This is likely because of the limited availability of sub-daily data (Berg *et al.* 2019). To our knowledge, our study is the first from both study regions that provides a detailed assessment of changes in hourly runoff extremes. In Figure 11, we indicate the relative change in flood magnitudes, considering the outputs of the hydrological model aggregated to daily values. For a 20-year return period flood, the ensemble average (both RCPs) projects an increase in daily runoff volumes by 13–20% in Alptal and by only 0–7% in Guanshan. The relative differences are about 30–50% lower than when the hourly flows are considered (Figure 11). Such change factors derived from daily flows are therefore not an appropriate reference for estimating the design flows for flood mitigation. Our results demonstrate the importance of considering hourly time steps when assessing the climate change impact on summer flood extremes in mountainous catchments.

The effect of the spatial scale is also important to consider when comparing our results with the findings of previous studies. Many floods in the Swiss catchment are

caused by convective precipitation events, which have a very limited spatial extent. Convective cells move over certain sites in a region but bypass others. Accordingly, intense thunderstorms in the Alptal catchment rarely lead to critical peak flows further downstream in the Sihl catchment (Ronco *et al.* 2015). It is therefore clear that mountain catchments are more affected by intensifying convective precipitation than downstream river sections. For the Rhine River at Maxau (catchment surface area 50,000 km^2), te Linde *et al.* (2010) projected an increase of the daily peak discharge of a 100-year flood by about 8–22% for 2036–2065 compared to 1961–1995, while the present study for the much smaller Alptal catchment projects an increase by 40–50% (Figure 11(b), daily values). Our results are in line with the findings of previous studies which indicate that the sensitivity of flood response to the temperature is greater for smaller catchments (Do *et al.* 2017; Sharma *et al.* 2018).

Uncertainty

We have summarized our results and the results of previous studies mostly by considering the ensemble average of a multi-climate-model analysis. Previous studies have confirmed that multi-model ensemble averages generally outperform individual RCMs (Park *et al.* 2016). However, the model spread is often substantial, reflecting both internal variability and climate model uncertainty.

In this study, we do find large differences between the outputs obtained from different model chains, in particular for the RCP 8.5 scenario and long return periods. In the Alptal catchment, for example, the hourly peak flow of a 100-year flood may increase by 3 to 275%, considering the 95% CI of the climate model ensemble. It is therefore clear that it is not possible to precisely predict by how much the extreme events will increase. However, the confidence that extreme flows will intensify is high, given that all GCM–RCM model chains lead to projections of positive changes.

The agreement between different model chains with respect to the direction of change is contrasting the results of numerous previous studies where the results were found to be dependent on the selected GCMs or RCMs (e.g., Camici *et al.* 2014). The use of hourly rather than daily time steps might explain the good agreement between different models on the direction of change. For example, for the RCP 4.5 scenario in the Guanshan catchment, all RCMs predict increasing magnitudes of hourly peak flows (Figure 11(a)), but for daily flows, the 60% CI regarding the changes in 100-year floods ranges between –23% and +85%. The confidence of the climate models in heavy precipitation intensification can be explained by a greater atmospheric water holding capacity with higher air temperatures according to the Clausius–Clapeyron relationship. Previous assessments for the Alpine region have shown that changes in extreme precipitation are approaching the Clausius–Clapeyron scaling (6–7% per degree warming) for hourly precipitation, but scale below the Clausius–Clapeyron rate for 1-day precipitation (Ban *et al.* 2018). The relevant changes in flood generation processes are therefore reflected much more clearly by hourly rather than daily time steps.

Due to the small signal to noise ratio in climate change impact studies on precipitation and extremes, previous authors have argued that it may suffice in many applications to consider just the natural climate variability of the current climate (Fatichi *et al.* 2016). Recent flood mitigation measures for the river Sihl (catchment surface area 343 km^2), to which the river Alp is a tributary, were planned without explicitly considering the possible impact of climate change on extremes. Instead, it was assumed that the potential threats of climate change can be handled by considering generous safety factors for the design floods, i.e., the upper limit of the 60% CI of the GEV fit to historical peak flow observations (Kleinn *et al.* 2019). However, the ensemble averages of our climate change impact simulations are in all cases (both study catchments, both RCPs) above the 60% CI of the GEV fit for the present climate (Figure 10). Of course, the statistical uncertainty of the GEV fit to the long stochastic data series is lower than the uncertainty of the GEV fit to relatively short historical data (Figure 7). In the Alptal catchment, however, a majority of the climate models projects extremes that are even above the upper limit of the 60% CI of the GEV fit to historical flows. For a 50-year flood, for example, the upper limit of the 60% CI is 32% higher than the fitted value (Figure 7(b)), while the ensemble average for 2021–2050 projects a 53% increase (both RCPs, Figure 11(b)). Given the huge damage potential of the river Sihl (Kleinn *et al.* 2019), we therefore recommend that potential climate change impacts on

extremes should be explicitly considered for flood mitigation.

In this study, we consider the uncertainties related to the climate models and climate scenarios. Among other sources of uncertainty that are not assessed here, the hydrological modelling uncertainty is perhaps the most important (Hall *et al.* 2014). The model structure and the model parameters may not equally apply to the present and the future conditions and already do not reproduce all storm types equally well for the current climate (Figure 4). Future studies should attempt to assess and quantify the role of hydrological modelling uncertainty for this type of applications, for example by choosing a parameter ensemble approach rather than considering only the best performing parameter set from the calibration.

CONCLUSIONS

Using the example of two forested headwater catchments in Switzerland and China, representing completely different climate zones, this study investigates how climate change will affect extreme summer flows in mountainous areas. Our results indicate a clear increase in flood frequencies and magnitudes in both catchments already in the near future (2021–2050). The high agreement between different model chains with respect to the direction of change is remarkable. The following reasons seem to have favoured the emergence of clear patterns of flood regime changes: (i) increasing the length of the climate data series using a weather generator reduces the statistical uncertainty when estimating low-probability flood peak events; (ii) rainfall events are intensifying in a warmer climate, but due to the relatively small spatial extent of convective storms, the effect on river peak flows is more significant at the scale of small headwater catchments; and (iii) modelling the response of mountain catchments to rainfall extremes requires hourly time steps, but most previous studies have used only daily time steps.

Despite the overall agreement regarding the intensification of extremes, the magnitude of change is highly uncertain. Detailed conclusions about the magnitude of future flood extremes are therefore not possible based on our results. However, a majority of the climate models project extremes that exceed the common safety factors for design floods. In our opinion, decision makers should therefore consider the possible impact of climate change for flood mitigation planning in mountain areas. Yet, detailed hydrological studies about floods in mountain areas are sparse even without considering the effect of climate change. This sparsity can be explained by the scarcity of rainfall and streamflow data from mountainous catchments. In this respect, the two studied locations in this study are pilot mountain research catchments in China and Switzerland where a relatively dense network of rain gauges has already been installed 10–20 years ago. Although these are short time scales in comparison to the return periods of large floods, the present study demonstrates that such records can be effectively used in combination with a weather generator and a hydrological model to estimate the magnitude and recurrence intervals of rare flood events. Our study thus underlines the importance of such data sets, which enable detailed flood hazard assessments required for flood mitigation purposes.

ACKNOWLEDGEMENTS

This study has been co-funded by the National Key R&D Program of China (2017YFC150250304), by the Yangtze River Commission and by the Swiss Federal Ministry of Environment (Sino-Swiss Pilot Project on Mountain Torrent Disaster Prevention). We are grateful to the National Centre for Climate Services (NCCS) for providing the CH2018 climate scenarios for Alptal and to the Federal Office of the Environment (FOEN) for the runoff data used in this study. We thank Tobias Siegfried for providing helpful comments on the manuscript.

AUTHOR CONTRIBUTIONS

S.R. designed and proposed the main structure of this research, analysed the data together with X.T. and G.Z and wrote the manuscript. H.W., P.Z. and M.S. organized and supervised the research and developed this study together with S.R. All authors discussed and reviewed the manuscript.

REFERENCES

Alfieri, L., Burek, P., Feyen, L. & Forzieri, G. 2015 Global warming increases the frequency of river floods in Europe. *Hydrol. Earth Syst. Sci.* **19**, 2247–2260. https://doi.org/10.5194/hess-19-2247-2015.

Allamano, P., Claps, P. & Laio, F. 2009 Global warming increases flood risk in mountainous areas. *Geophys. Res. Lett.* **36**, 1–5. https://doi.org/10.1029/2009gl041395.

Almasi, P. & Soltani, S. 2017 Assessment of the climate change impacts on flood frequency (case study: Bazoft Basin, Iran). *Stoch. Environ. Res. Risk Assess.* **31**, 1171–1182. https://doi.org/10.1007/s00477-016-1263-1.

Andres, N. & Badoux, A. 2018 The Swiss flood and landslide damage database: normalisation and trends. *J. Flood Risk Manag.* 1–12. https://doi.org/10.1111/jfr3.12510.

Arnell, N. W. & Gosling, S. N. 2016 The impacts of climate change on river flood risk at the global scale. *Clim. Change* **134**, 387–401. https://doi.org/10.1007/s10584-014-1084-5.

Asadi, P., Engelke, S. & Davison, A. C. 2018 Optimal regionalization of extreme value distributions for flood estimation. *J. Hydrol.* **556**, 182–193. https://doi.org/10.1016/j.jhydrol.2017.10.051.

Ban, N., Rajczak, J., Schmidli, J. & Schär, C. 2018 Analysis of alpine precipitation extremes using generalized extreme value theory in convection-resolving climate simulations. *Clim. Dyn.* **0**, 1–15. https://doi.org/10.1007/s00382-018-4339-4.

Berg, P., Christensen, O. B., Klehmet, K., Lenderink, G., Olsson, J., Teichmann, C. & Yang, W. 2019 Summertime precipitation extremes in a EURO-CORDEX 0.11° ensemble at an hourly resolution. *Nat. Hazards Earth Syst. Sci.* **19**, 957–971. https://doi.org/10.5194/nhess-19-957-2019.

Bordoy, R. & Burlando, P. 2014a Stochastic downscaling of precipitation to high-resolution scenarios in orographically complex regions: 1. Model evaluation. *Water Resour. Res.* **50**, 540–561. https://doi.org/10.1002/2012WR013289.

Bordoy, R. & Burlando, P. 2014b Stochastic downscaling of climate model precipitation outputs in orographically complex regions: 2. Downscaling methodology. *Water Resour. Res.* **50**, 562–579. https://doi.org/10.1002/wrcr.20443.

Burton, A., Kilsby, C. G., Fowler, H. J., Cowpertwait, P. S. P. & O'Connell, P. E. 2008 RainSim: a spatial–temporal stochastic rainfall modelling system. *Environ. Model. Softw.* **23**, 1356–1369. https://doi.org/10.1016/j.envsoft.2008.04.003.

Camici, S., Brocca, L., Melone, F. & Moramarco, T. 2014 Impact of climate change on flood frequency using different climate models and downscaling approaches. *J. Hydrol. Eng.* **19**, 04014002. https://doi.org/10.1061/(asce)he.1943-5584.0000959.

CCCPC (Central Committee of the Communist Party of China) 2015 The 13th Five-Year Plan for Economic and Social Development of the People's Republic of China (2016–2020).

Cowpertwait, P. S. P. 1995 A generalized spatial-temporal model of rainfall based on a clustered point process. *Proc. – R. Soc. London, A* **450**, 163–175. https://doi.org/10.1098/rspa.1995.0077.

Cowpertwait, P. S. P., Kilsby, C. G. & O'Connell, P. E. 2002 A space-time Neyman–Scott model of rainfall: empirical analysis of extremes. *Water Resour. Res.* **38**, 6-1–6-14. https://doi.org/10.1029/2001wr000709.

Dankers, R. & Feyen, L. 2008 Climate change impact on flood hazard in Europe: an assessment based on high-resolution climate simulations. *J. Geophys. Res. Atmos.* **113**, 1–17. https://doi.org/10.1029/2007JD009719.

Dankers, R. & Feyen, L. 2009 Flood hazard in Europe in an ensemble of regional climate scenarios. *J. Geophys. Res. Atmos.* **114**, 1–16. https://doi.org/10.1029/2008JD011523.

David, O., Ascough II, J. C., Leavesley, G. H. & Ahuja, L. R., 2010 Rethinking modeling framework design: Object Modeling System 3.0. In: *Modelling for Environment's Sake, Proceedings 5th Biennial Conference International Environmental Modelling and Software Society,* Ottawa, Canada, February 2010, pp. 1190–1198.

Ding, Y. 1992 Summer monsoon rainfalls in China. *J. Meteorol. Soc. Japan. Ser. II* **70**, 373–396. https://doi.org/10.2151/jmsj1965.70.1b_373.

Do, H. X., Westra, S. & Leonard, M. 2017 A global-scale investigation of trends in annual maximum streamflow. *J. Hydrol.* **552**, 28–43. https://doi.org/10.1016/j.jhydrol.2017.06.015.

Duan, Q. Y., Gupta, V. K. & Sorooshian, S. 1993 Shuffled complex evolution approach for effective and efficient global minimization. *J. Optim. Theory Appl.* **76**, 501–521. https://doi.org/10.1007/BF00939380.

Fatichi, S., Ivanov, V. Y. & Caporali, E. 2011 Simulation of future climate scenarios with a weather generator. *Adv. Water Resour.* **34**, 448–467. https://doi.org/10.1016/j.advwatres.2010.12.013.

Fatichi, S., Rimkus, S., Burlando, P., Bordoy, R. & Molnar, P. 2015 High-resolution distributed analysis of climate and anthropogenic changes on the hydrology of an Alpine catchment. *J. Hydrol.* **525**, 362–382. https://doi.org/10.1016/j.jhydrol.2015.03.036.

Fatichi, S., Vivoni, E. R., Ogden, F. L., Ivanov, V. Y., Mirus, B., Gochis, D., Downer, C. W., Camporese, M., Davison, J. H., Ebel, B., Jones, N., Kim, J., Mascaro, G., Niswonger, R., Restrepo, P., Rigon, R., Shen, C., Sulis, M. & Tarboton, D. 2016 An overview of current applications, challenges, and future trends in distributed process-based models in hydrology. *J. Hydrol.* **537**, 45–60. https://doi.org/10.1016/j.jhydrol.2016.03.026.

Fischer, S. & Schumann, A. 2019 Spatio-temporal consideration of the impact of flood event types on flood statistic. *Stoch. Environ. Res. Risk Assess.* **2**. https://doi.org/10.1007/s00477-019-01690-2.

Fischer, E. M., Beyerle, U. & Knutti, R. 2013 Robust spatially aggregated projections of climate extremes. *Nat. Clim. Chang.* **3**, 1033–1038. https://doi.org/10.1038/nclimate2051.

François, B., Schlef, K. E., Wi, S. & Brown, C. M. 2019 Design considerations for riverine floods in a changing climate – a review. *J. Hydrol.* **574**, 557–573. https://doi.org/10.1016/j.jhydrol.2019.04.068.

Gao, C., He, Z., Pan, S., Xuan, W. & Xu, Y. P. 2018 Effects of climate change on peak runoff and flood levels in Qu River Basin, East China . *J. Hydro-Environment Res.* 1–14. https://doi.org/10.1016/j.jher.2018.02.005.

Giorgi, F., Jones, C. & Asrar, G. R. 2009 Addressing climate information needs at the regional level: the CORDEX framework. *World Meteorol. Organ. Bull.* **58**, 175–183. https://doi.org/10.1109/ICASSP.2009.4960141.

Gobiet, A., Kotlarski, S., Beniston, M., Heinrich, G., Rajczak, J. & Stoffel, M. 2014 21st century climate change in the European Alps – a review. *Sci. Total Environ.* **493**, 1138–1151. https://doi.org/10.1016/j.scitotenv.2013.07.050.

Gu, H., Yu, Z., Yang, C. & Ju, Q. 2018 Projected changes in hydrological extremes in the Yangtze River Basin with an ensemble of regional climate simulations. *Water* **10**, 1279. https://doi.org/10.3390/w10091279.

Gudmundsson, L., Bremnes, J. B., Haugen, J. E. & Engen-Skaugen, T. 2012 Technical note: downscaling RCM precipitation to the station scale using statistical transformations – a comparison of methods. *Hydrol. Earth Syst. Sci.* **16**, 3383–3390. https://doi.org/10.5194/hess-16-3383-2012.

Hall, J., Arheimer, B., Borga, M., Brázdil, R., Claps, P., Kiss, A., Kjeldsen, T. R., Kriaučiūnienė, J., Kundzewicz, Z. W., Lang, M., Llasat, M. C., Macdonald, N., McIntyre, N., Mediero, L., Merz, B., Merz, R., Molnar, P., Montanari, A., Neuhold, C., Parajka, J., Perdigão, R. A. P., Plavcová, L., Rogger, M., Salinas, J. L., Sauquet, E., Schär, C., Szolgay, J., Viglione, A. & Blöschl, G. 2014 Understanding flood regime changes in Europe: a state-of-the-art assessment. *Hydrol. Earth Syst. Sci.* **18**, 2735–2772. https://doi.org/10.5194/hess-18-2735-2014.

Hashmi, M. Z., Shamseldin, A. Y. & Melville, B. W. 2011 Comparison of SDSM and LARS-WG for simulation and downscaling of extreme precipitation events in a watershed. *Stoch. Environ. Res. Risk Assess.* **25**, 475–484. https://doi.org/10.1007/s00477-010-0416-x.

Hirabayashi, Y., Mahendran, R., Koirala, S., Konoshima, L., Yamazaki, D., Watanabe, S., Kim, H. & Kanae, S. 2013 Global flood risk under climate change. *Nat. Clim. Chang.* **3**, 816–821. https://doi.org/10.1038/nclimate1911.

Iturbide, M., Bedia, J., Herrera, S., Baño-Medina, J., Fernández, J., Frías, M. D., Manzanas, R., San-Martín, D., Cimadevilla, E., Cofiño, A. S. & Gutiérrez, J. M. 2019 The R-based climate4R open framework for reproducible climate data access and post-processing. *Environ. Model. Softw.* **111**, 42–54. https://doi.org/10.1016/j.envsoft.2018.09.009.

Keller, D. E., Fischer, A. M., Liniger, M. A., Appenzeller, C. & Knutti, R. 2017 Testing a weather generator for downscaling climate change projections over Switzerland. *Int. J. Climatol.* **37**, 928–942. https://doi.org/10.1002/joc.4750.

Keller, L., Rössler, O., Martius, O. & Weingartner, R. 2019 Comparison of scenario-neutral approaches for estimation of climate change impacts on flood characteristics. *Hydrol. Process.* **33**, 535–550. https://doi.org/10.1002/hyp.13341.

Khazaei, M. R., Zahabiyoun, B. & Saghafian, B. 2012 Assessment of climate change impact on floods using weather generator and continuous rainfall-runoff model. *Int. J. Climatol.* **32**, 1997–2006. https://doi.org/10.1002/joc.2416.

Kleinn, J., Aller, D., Zappa, M., Andres, N., Bresch, D., Marti, C. & Oplatka, M. 2019 Kontinuierliche Wirkungsabschätzung von verschiedenen Hochwasserschutzmaßnahmen überdas gesamte Abfluss-Spektrum am Beispiel der Sihl. *Hydrol. und Wasserbewirtschaftung* **63**, 158–167. https://doi.org/10.5675/HyWa_2019.3_3.

Köplin, N., Schädler, B., Viviroli, D. & Weingartner, R. 2014 Seasonality and magnitude of floods in Switzerland under future climate change. *Hydrol. Process.* **28**, 2567–2578. https://doi.org/10.1002/hyp.9757.

Leavesley, G. H. & Stannard, L. G. 1995 The precipitation-runoff modeling system – PRMS. In: *Computer Models of Watershed Hydrology* (V. P. Singh, ed.). Water Resources Publications, Highlands Ranch, CO, pp. 281–310.

Leavesley, G. H., Markstrom, S. L., Viger, R. J. & Hay, L. E. 2006 USGS Modular Modeling System (MMS)–Precipitation-Runoff Modeling System (PRMS) MMS–PRMS. In: *Watershed Models* (V. Singh & D. Frevert, eds). CRC Press, Boca Raton, FL, pp. 159–177.

Machado, M. J., Botero, B. A., López, J., Francés, F., Díez-Herrero, A. & Benito, G. 2015 Flood frequency analysis of historical flood data under stationary and non-stationary modelling. *Hydrol. Earth Syst. Sci.* **19**, 2561–2576. https://doi.org/10.5194/hess-19-2561-2015.

Madsen, H., Lawrence, D., Lang, M., Martinkova, M. & Kjeldsen, T. R. 2014 Review of trend analysis and climate change projections of extreme precipitation and floods in Europe. *J. Hydrol.* **519**, 3634–3650. https://doi.org/10.1016/j.jhydrol.2014.11.003.

Marchi, L., Borga, M., Preciso, E. & Gaume, E. 2010 Characterisation of selected extreme flash floods in Europe and implications for flood risk management. *J. Hydrol.* **394**, 118–133. https://doi.org/10.1016/j.jhydrol.2010.07.017.

Mekonnen, D. F. & Disse, M. 2018 Analyzing the future climate change of Upper Blue Nile River Basin (UBNRB) using statistical down scaling techniques. *Hydrol. Earth Syst. Sci.* **22**, 2391–2408. https://doi.org/10.5194/hess-22-2391-2018.

Milly, P. C. D., Betancourt, J., Falkenmark, M., Hirsch, R. M., Kundzewicz, Z. W., Lettenmaier, D. P. & Stouffer, R. J. 2005 Stationarity is dead: whither water management? *Science* **319**, 573–574. https://doi.org/10.1126/science.1151915.

National Centre for Climate Services 2018 *CH2018 – Climate Scenarios for Switzerland*. Zurich, Switzerland.

Olsen, J. R. 2006 Climate change and floodplain management in the United States. *Clim. Change* **76**, 407–426. https://doi.org/10.1007/s10584-005-9020-3.

Park, C., Min, S. K., Lee, D., Cha, D. H., Suh, M. S., Kang, H. S., Hong, S. Y., Lee, D. K., Baek, H. J., Boo, K. O. & Kwon, W. T. 2016 Evaluation of multiple regional climate models for

summer climate extremes over East Asia. *Clim. Dyn.* **46**, 2469–2486. https://doi.org/10.1007/s00382-015-2713-z.

Paschalis, A., Fatichi, S., Molnar, P., Rimkus, S. & Burlando, P. 2014 On the effects of small scale space-time variability of rainfall on basin flood response. *J. Hydrol.* **514**, 313–327. https://doi.org/10.1016/j.jhydrol.2014.04.014.

Peleg, N., Blumensaat, F., Molnar, P., Fatichi, S. & Burlando, P. 2017a Partitioning the impacts of spatial and climatological rainfall variability in urban drainage modeling. *Hydrol. Earth Syst. Sci.* **21**, 1559–1572. https://doi.org/10.5194/hess-21-1559-2017.

Peleg, N., Fatichi, S., Paschalis, A., Molnar, P. & Burlando, P. 2017b An advanced stochastic weather generator for simulating 2-D high-resolution climate variables. *J. Adv. Model. Earth Syst.* **9**, 1595–1627. https://doi.org/10.1002/2016MS000854.

Prudhomme, C., Jakob, D. & Svensson, C. 2003 Uncertainty and climate change impact on the flood regime of small UK catchments. *J. Hydrol.* **277**, 1–23. https://doi.org/10.1016/S0022-1694(03)00065-9.

Ragettli, S., Pellicciotti, F., Bordoy, R. & Immerzeel, W. W. 2013 Sources of uncertainty in modeling the glaciohydrological response of a Karakoram watershed to climate change. *Water Resour. Res.* **49**, 6048–6066. https://doi.org/10.1002/wrcr.20450.

Ragettli, S., Immerzeel, W. W. & Pellicciotti, F. 2016 Contrasting climate change impact on river flows from high-altitude catchments in the Himalayan and Andes Mountains. *Proc. Natl. Acad. Sci. U.S.A.* **113**, 9222–9227. https://doi.org/10.1073/pnas.1606526113.

Ragettli, S., Zhou, J., Wang, H., Liu, C. & Guo, L. 2017 Modeling flash floods in ungauged mountain catchments of China: a decision tree learning approach for parameter regionalization. *J. Hydrol.* **555**, 330–346. https://doi.org/10.1016/j.jhydrol.2017.10.031.

Rajczak, J. & Schär, C. 2017 Projections of future precipitation extremes over Europe: a multimodel assessment of climate simulations. *J. Geophys. Res. Atmos.* **122**, 10,773–10,800. https://doi.org/10.1002/2017JD027176.

Rajczak, J., Pall, P. & Schär, C. 2013 Projections of extreme precipitation events in regional climate simulations for Europe and the alpine region. *J. Geophys. Res. Atmos.* **118**, 3610–3626. https://doi.org/10.1002/jgrd.50297.

Riahi, K., Rao, S., Krey, V., Cho, C., Chirkov, V., Fischer, G., Kindermann, G., Nakicenovic, N. & Rafaj, P. 2011 RCP 8.5 – a scenario of comparatively high greenhouse gas emissions. *Clim. Change* **109**, 33–57. https://doi.org/10.1007/s10584-011-0149-y.

Ronco, P., Bullo, M., Torresan, S., Critto, A., Olschewski, R., Zappa, M. & Marcomini, A. 2015 KULTURisk regional risk assessment methodology for water-related natural hazards – Part 2: application to the Zurich case study. *Hydrol. Earth Syst. Sci.* **19**, 1561–1576. https://doi.org/10.5194/hess-19-1561-2015.

Rosenberg, E. A., Keys, P. W., Booth, D. B., Hartley, D., Burkey, J., Steinemann, A. C. & Lettenmaier, D. P. 2010 Precipitation extremes and the impacts of climate change on stormwater infrastructure in Washington State. *Clim. Change* **102**, 319–349. https://doi.org/10.1007/s10584-010-9847-0.

Scherrer, S. C., Fischer, E. M., Posselt, R., Liniger, M. A., Croci-Maspoli, M. & Knutti, R. 2016 Emerging trends in heavy precipitation and hot temperature extremes in Switzerland. *J. Geophys. Res.* **121**, 2626–2637. https://doi.org/10.1002/2015JD024634.

Serinaldi, F. & Kilsby, C. G. 2015 Stationarity is undead: uncertainty dominates the distribution of extremes. *Adv. Water Resour.* **77**, 17–36. https://doi.org/10.1016/j.advwatres.2014.12.013.

Sharma, A., Wasko, C. & Lettenmaier, D. P. 2018 If precipitation extremes are increasing, why aren't floods? *Water Resour. Res.* **54**, 8545–8551. https://doi.org/10.1029/2018WR023749.

Sunyer, M. A., Madsen, H. & Ang, P. H. 2012 A comparison of different regional climate models and statistical downscaling methods for extreme rainfall estimation under climate change. *Atmos. Res.* **103**, 119–128. https://doi.org/10.1016/j.atmosres.2011.06.011.

te Linde, A. H., Aerts, J. C. J. H., Bakker, A. M. R. & Kwadijk, J. C. J. 2010 Simulating low-probability peak discharges for the Rhine basin using resampled climate modeling data. *Water Resour. Res.* **46**, 1–19. https://doi.org/10.1029/2009WR007707.

Thomson, A. M., Calvin, K. V., Smith, S. J., Kyle, G. P., Volke, A., Patel, P., Delgado-Arias, S., Bond-Lamberty, B., Wise, M. A., Clarke, L. E. & Edmonds, J. A. 2011 RCP4.5: a pathway for stabilization of radiative forcing by 2100. *Clim. Change* **109**, 77–94. https://doi.org/10.1007/s10584-011-0151-4.

Tian, Y., Xu, Y.-P., Booij, M. J. & Cao, L. 2016 Impact assessment of multiple uncertainty sources on high flows under climate change. *Hydrol. Res.* **47**, 61–74. https://doi.org/10.2166/nh.2015.008.

Vallam, P. & Qin, X. S. 2016 Multi-site rainfall simulation at tropical regions: a comparison of three types of generators. *Meteorol. Appl.* **23**, 425–437. https://doi.org/10.1002/met.1567.

van der Wiel, K., Wanders, N., Selten, F. M. & Bierkens, M. F. P. 2019 Added value of large ensemble simulations for assessing extreme river discharge in a 2°C warmer world. *Geophys. Res. Lett.* **46**, 2093–2102. https://doi.org/10.1029/2019GL081967.

Westra, S., Fowler, H. J., Evans, J. P., Alexander, L. V., Berg, P., Johnson, F., Kendon, E. J., Lenderink, G. & Roberts, N. M. 2014 Future changes to the intensity and frequency of short-duration extreme rainfall. *Rev. Geophys.* https://doi.org/10.1002/2014RG000464

Wheater, H. S., Chandler, R. E., Onof, C. J., Isham, V. S., Bellone, E., Yang, C., Lekkas, D., Lourmas, G. & Segond, M. L. 2005 Spatial-temporal rainfall modelling for flood risk estimation. *Stoch. Environ. Res. Risk Assess.* **19**, 403–416. https://doi.org/10.1007/s00477-005-0011-8.

Wilks, D. S. & Wilby, R. L. 1999 The weather generation game: a review of stochastic weather models. *Prog. Phys. Geogr.* **23**, 329–357. https://doi.org/10.1191/030913399666525256.

Yates, D. N., Warner, T. T. & Leavesley, G. H. 2000 Prediction of a flash flood in complex terrain. Part II: a comparison of flood discharge simulations using rainfall input from radar, a dynamic model, and an automated algorithmic system. *J. Appl. Meteorol.* **39**, 815–825. https://doi.org/10.1175/1520-0450(2000)039<0815:POAFFI>2.0.CO;2.

Zhai, X., Liu, R., Yang, Y., Bi, Q. & Liu, Q. 2017 Flash flood warning-oriented hydrometric network optimal design. *J. Geo-Information Sci.* **19**, 1634–1642. https://doi.org/10.3724/SP.J.1047.2017.01634.

Zhang, Q., Xu, C. Y., Zhang, Z., Chen, Y. D., Liu, C. l. & Lin, H. 2008 Spatial and temporal variability of precipitation maxima during 1960–2005 in the Yangtze River Basin and possible association with large-scale circulation. *J. Hydrol.* **353**, 215–227. https://doi.org/10.1016/j.jhydrol.2007.11.023.

First received 31 July 2019; accepted in revised form 27 November 2019. Available online 18 December 2019